

Supporting Information for

C-terminal glycine-gated radical initiation by GTP 3',8-cyclase in the molybdenum cofactor biosynthesis.

Bradley M. Hover[†] and Kenichi Yokoyama^{†}*

[†] Department of Biochemistry, Duke University Medical Center, Durham, NC, 27710.

*Corresponding Author: ken.yoko@duke.edu,

Table of Contents

Supplementary Methods

Analysis of MoaA for PTM, Anaerobic SEC Analysis, Functional Characterization of MoaA with [3'-D]GTP

Supplementary Figures

Figure S1. Biochemical Characterization of MoaA GG Motif Mutants

Figure S2. ITC Analysis for Substrate Binding to MoaA GG Motif Mutants

Figure S3. KIE in the wt- and G340A-MoaA catalysis

Figure S4. MS Analysis of the MoaA C-terminal tail

Figure S5. Deuterium transfer from GTP to 5'-dA in wt- and G340A-MoaA

Figure S6. Structural Comparison of Radical SAM Enzymes

Figure S7. Loops around the active-site of MoaA

Supplementary Tables

Table S1. Complete List of the Steady State Kinetic Parameters for MoaA mutants

Table S2. PCR Primers for MoaA GG Motif Mutants

Supplementary Methods

Analysis of MoaA for PTM

MoaA (540 $\mu\text{g/mL}$) in 50 mM ammonium bicarbonate pH 8.0 was treated with 25 $\mu\text{g/mL}$ trypsin for 24 hours at 37°C. The digested sample was filtered with a 10,000 Da MWCO filter, lyophilized, and resuspended in water. 5 μL of 50 μM digested peptide was analyzed in positive ion-mode using an Agilent ESI-TOF-MS and Agilent Poroshell 120, C18, 2.1 x 75 mm, 2.7 μm column (Part No #697775-906). Chromatography was performed with at a flow rate of 0.3 mL/min using a linear gradient of 2-24% acetonitrile in water for 20 min. Data was analyzed using Agilent Masshunter software.

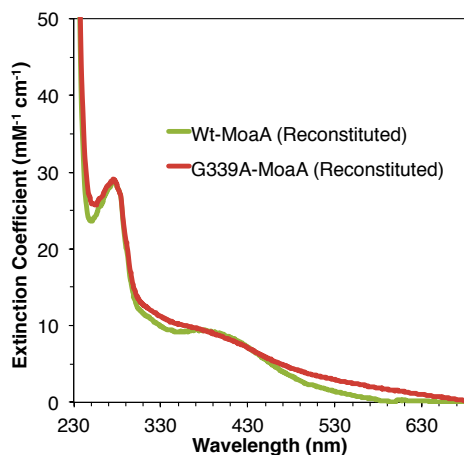
Anaerobic Size Exclusion Chromatography

MoaA (200 μL of 75 μM) was analyzed at 4 °C under anaerobic conditions by fast protein liquid chromatography (ATKA) using a GE Superdex 200 10/300 GL column (Part Number # 17-5175-01). An isocratic gradient at 3 mL/min was employed using an anaerobic buffer: 50 mM Tris-HCl (pH 7.6), 300 mM NaCl, 5 mM DTT, 1 mM MgCl_2 . Protein elution was monitored by absorbance at 280 nm. Elution containing MoaA were collected under the flow of argon gas and analyzed by SDS-PAGE and for activity, as described above. For analysis in the presence of substrates, 0.1 mM GTP and SAM was added to the mobile phase. A similar protocol was used for analyzing the MoaA GG motif mutants.

MS characterization of 5'-dA produced in the reactions with [3'-D]GTP

To determine the amount of deuterium atom incorporation into 5'-dA, the MoaA assay was performed in the presence of 30 μM wt- or G340A-MoaA, 60 μM MoaC, 0.5 mM SAM, 0.5 mM GTP or [3'-D]GTP, and with or without 0.5 mM 11-mer peptide. Reactions were filtered with a 10,000 Da MWCO filter, purified using SP-Sepharose resin (NH_4^+ form) to remove reaction contaminants, and then analyzed in positive ion-mode using an Agilent ESI-TOF-MS and Agilent Poroshell 120, C18, 2.1 x 75 mm, 2.7 μm column (Part No #697775-906). A linear gradient was employed at 0.2 mL/min using 30 mM ammonium formate, pH 4.5 (Solvent A) and 100% ACN (Solvent B): 2-85% B for 20 min. Data was analyzed using Agilent Masshunter software. The percent incorporation of deuterium was calculated based on: $100 \times ([\text{MS Intensity at } m/z \text{ 253.1}]) / ([\text{MS Intensity at } m/z \text{ 253.1}] + [\text{MS Intensity at } m/z \text{ 252.1}])$.

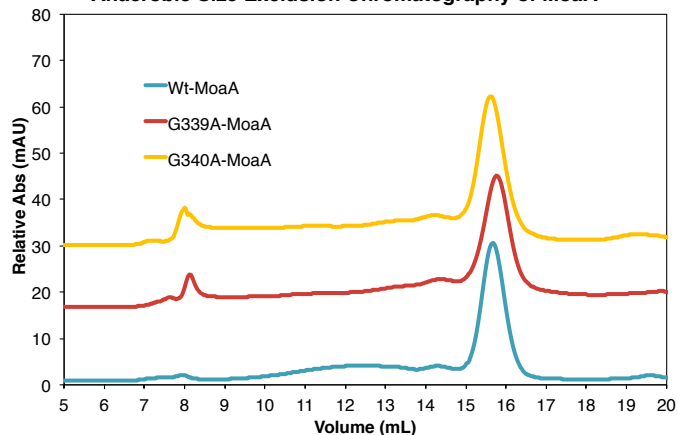
(a) UV-vis Absorption Spectra of Reconstituted MoaA



(b) Summary of [4Fe-4S] Cluster Content in MoaA Mutants After *In vitro* Reconstitution

Enzyme	[4Fe-4S] Cluster per Protein Monomer
MoaA Wt	2.13 ± 0.03
MoaA Δ330-340	1.62 ± 0.06
MoaA Δ336-340	1.99 ± 0.11
MoaA G339A	1.92 ± 0.06
MoaA G339S	1.64 ± 0.03
MoaA G339V	1.31 ± 0.02
MoaA G340A	1.87 ± 0.05
MoaA G340S	1.79 ± 0.08
MoaA G340V	1.34 ± 0.01
Avg for GG Mutants	1.69 ± 0.26

(c) Anaerobic Size Exclusion Chromatography of MoaA



(d) Anaerobic Size Exclusion Chromatography of MoaA

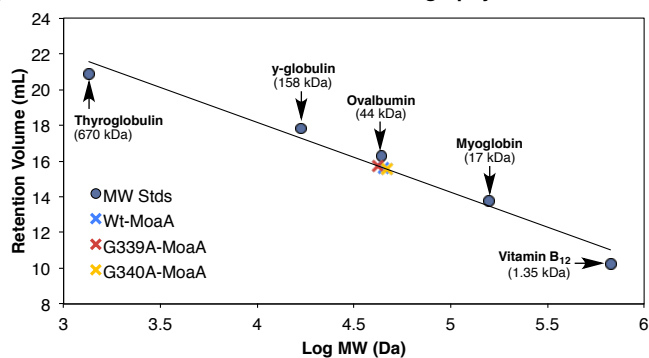


Figure S1. Characterization of MoaA GG-Motif Mutants. (a), UV-Vis Spectra of wt- and G339A-MoaA before and after anaerobic *in vitro* reconstitution of Fe-S Clusters. (b) Fe-S cluster content for each of the MoaA GG-motif mutants after reconstitution based on previously described ferrozine assay.¹ (c) and (d) Size exclusion column chromatography of wt-MoaA and MoaA GG-motif mutants in the presences of 0.1 mM SAM and GTP. MoaA and all tested MoaA variants eluted at 44.6 ± 2.1 kDa min regardless of the anaerobic condition or presence of substrates.

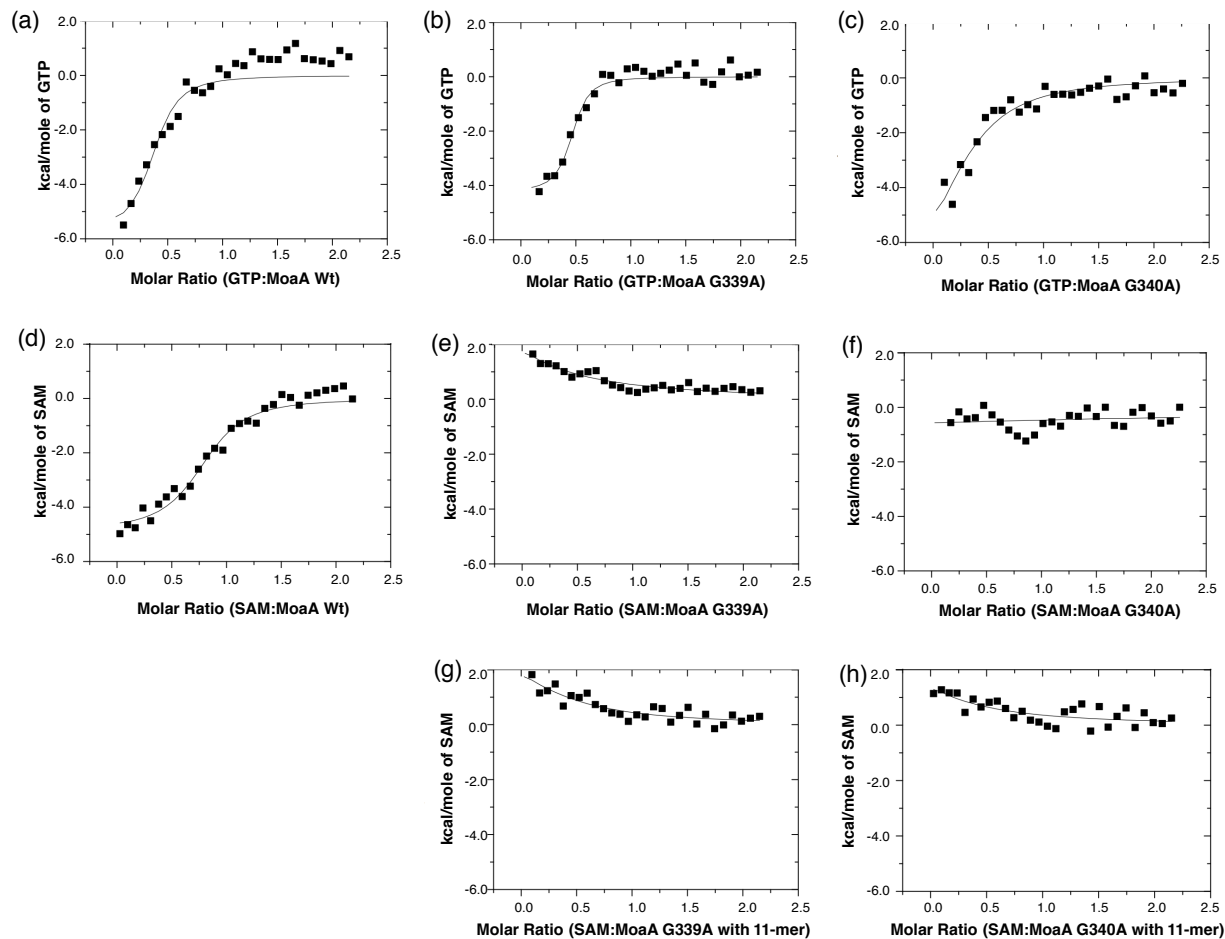


Figure S2. ITC Analysis for Substrate Binding to MoaA GG Motif Mutants. Representative plots of anaerobic ITC experiments using 35 μ M MoaA in 20 mM Tris, pH 7.6, 150 mM NaCl, 5 mM DTT titrated with 350 μ M substrates in an identical buffer. (a) Wt-MoaA titrated with GTP. (b) G339A-MoaA titrated with GTP. (c) G340A-MoaA titrated with GTP. (d) Wt-MoaA titrated with SAM. (e) G339A-MoaA titrated with SAM. (f) G340A-MoaA titrated with SAM. (g) G339A-MoaA and 0.5 mM 11-mer Wt peptide titrated with SAM. (h) G340A-MoaA and 0.5 mM 11-mer Wt titrated with SAM.

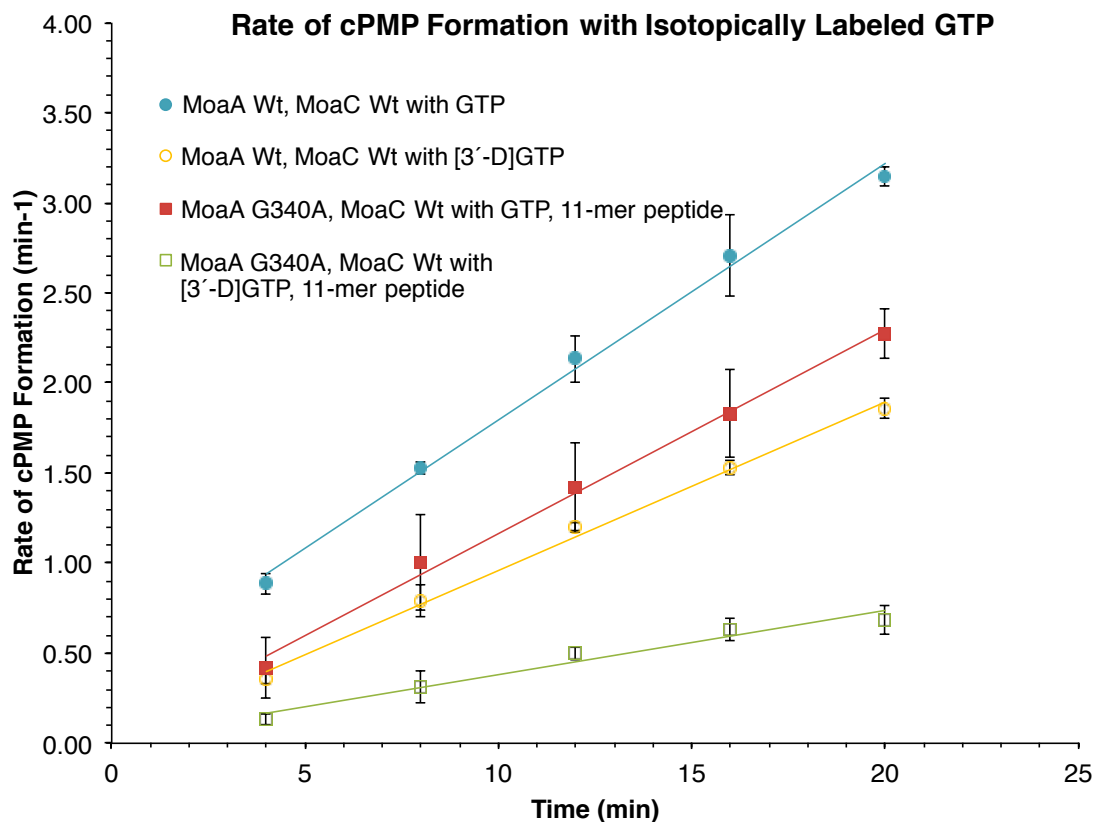


Figure S3. KIE in the wt- and G340A-MoaA catalysis. Rate of cPMP formation, in min^{-1} , for wt-MoaA and G340A-MoaA using GTP or $[3\text{'-D}]$ GTP. MoaA ($3\ \mu\text{M}$) was assayed in the presence of $10\ \mu\text{M}$ MoaC, $1\ \text{mM}$ SAM, $1\ \text{mM}$ DTH, $5\ \text{mM}$ DTT, $2\ \text{mM}$ MgCl_2 , $0.3\ \text{mM}$ NaCl and $1\ \text{mM}$ GTP or $[3\text{'-D}]$ GTP in $50\ \text{mM}$ Tris-HCl (pH 7.6) over 20 minutes at $25\ ^\circ\text{C}$. Reactions were performed in triplicated, and the error bars represent standard deviations.

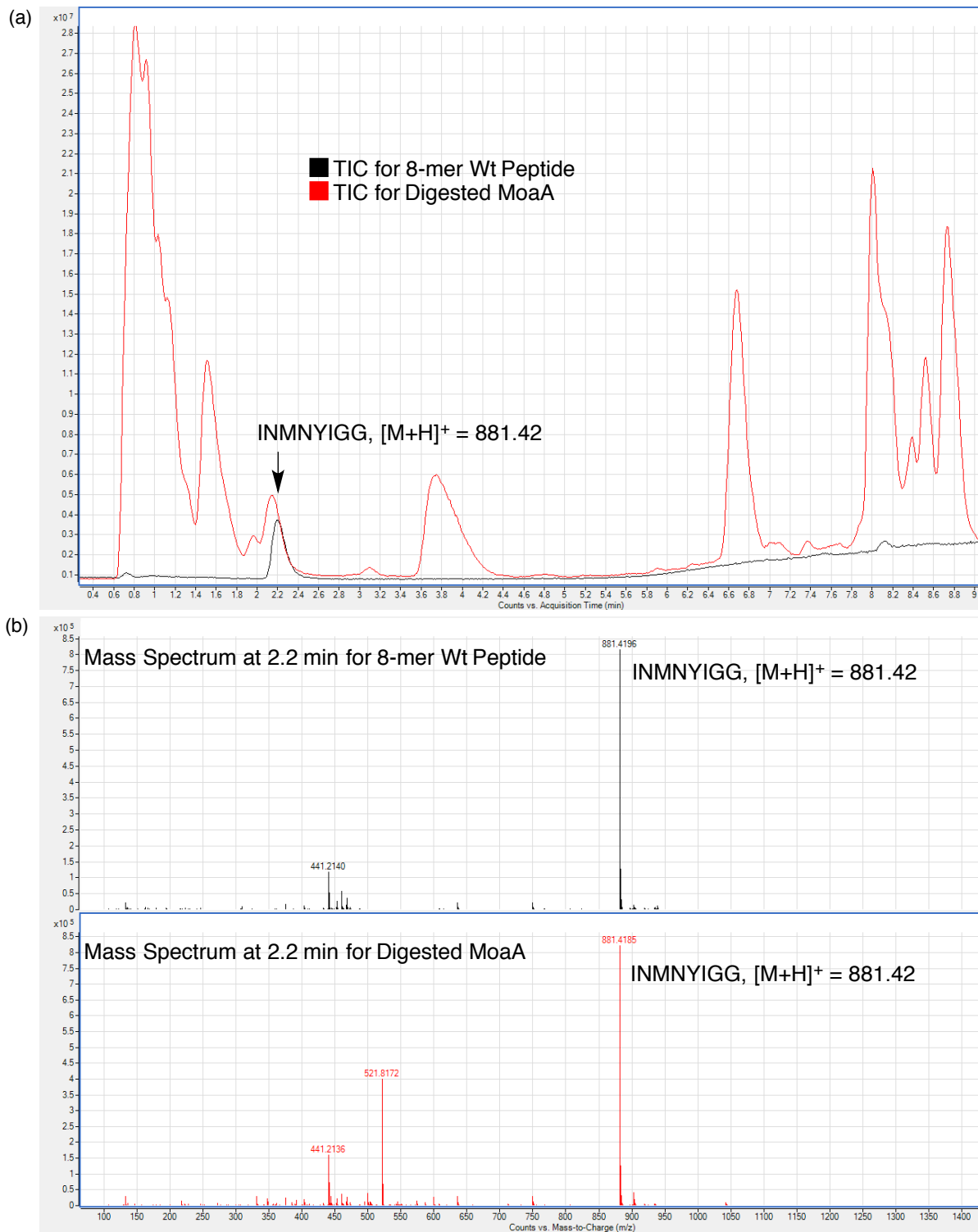


Figure S4. MS Analysis of the MoaA C-terminal tail. (a) Total ion chromatography from positive-ion LC-MS analysis of 50 μ M trypsin-digested wt-MoaA (red trace) and 50 μ M 8-mer synthetic peptide standard (black trace, INMNYIGG, $[M+H]^+ = 881.420$). The position of elution of the unmodified C-terminal tail is indicated with arrow. (b) Mass spectra of the trypsin digested wt-MoaA (top) and the 8-mer synthetic peptide (bottom). Analysis of the digested wt MoaA indicated only the unmodified C-terminal fragment, $[M+H]^+ = 881.419$. No posttranslational modification common in ubiquitin-like proteins, such as adenylation (+329 m/z), sulfation (+16 m/z) or amidation (-58 m/z), was detected.

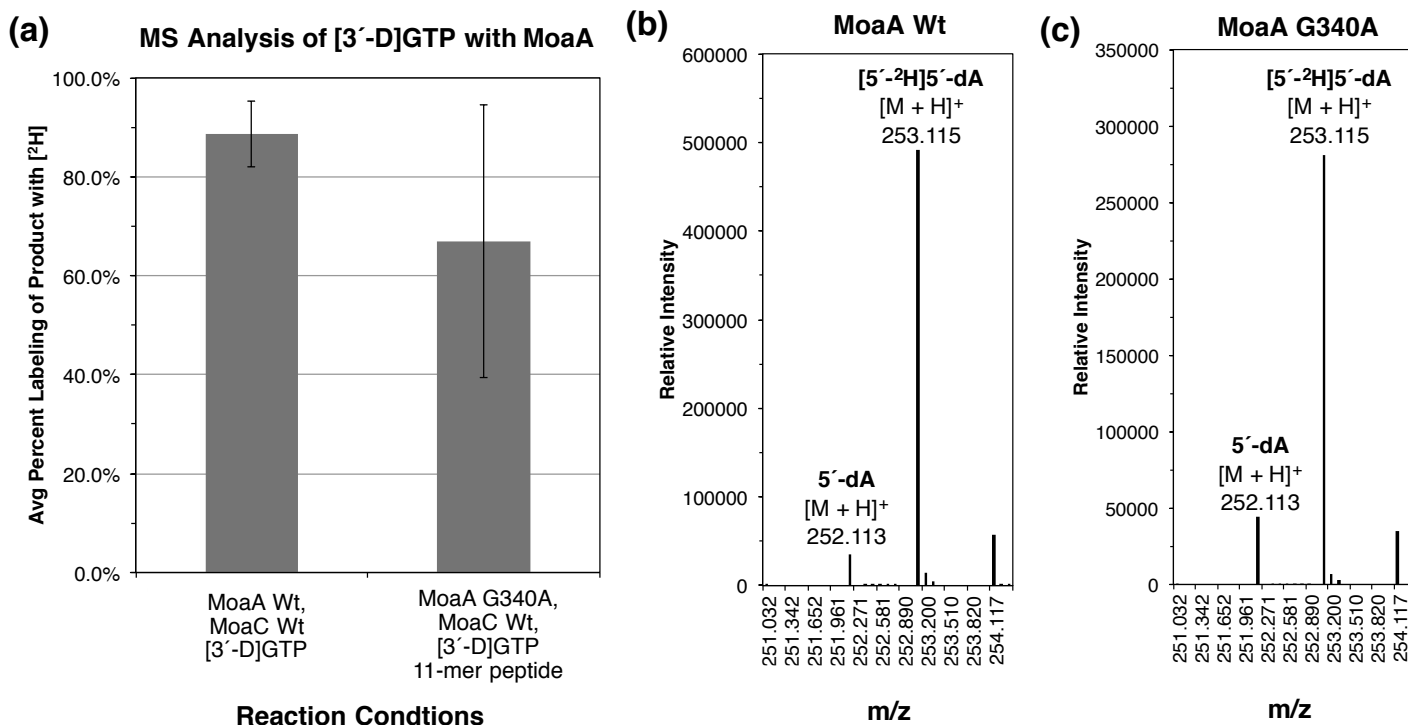


Figure S5. Deuterium transfer from GTP to 5'-dA in wt- and G340A-MoaA. To investigate the previously discussed possibility that the GG motif as the site of glycy radical formation, the transfer of the deuterium atom from the 3'-position of GTP to 5'-dA was studied in the wt-MoaA and in the G340A-MoaA complemented with the 11-mer peptide. The assays were performed using 30 μM wt-MoaA or 30 μM G340A-MoaA complemented with 0.5 mM 11-mer peptide in the presence of 60 μM wt-MoaC, 0.5 mM SAM, and 0.5 mM [3'-D]GTP. The G340A assay uses large excess of the peptide relative to the enzyme. Under this condition, if glycy radical is formed on the peptide and abstracts a deuterium atom from the 3'-position of GTP, the deuterium will be transferred to the peptide and not 5'-dA. (a) Average % incorporation of deuterium into 5'-dA. The % incorporation was determined based on the ratio between the intensities of the signals at m/z 252.1 and 253.1 in the LC-MS analysis of 5'-dA produced by the MoaA assays. (b and c) Representative Mass Spectra of 5'-dA from assays with wt-MoaA (b) and with G340A-MoaA complemented with the 11-mer peptide (c). These analyses suggest that nearly all of the detected 5'-dA had ^2H incorporated even in the presence of large excess of the peptide. Based on these observations, our data suggests that the GG motif in MoaA does not provide the site of glycy radical formation.

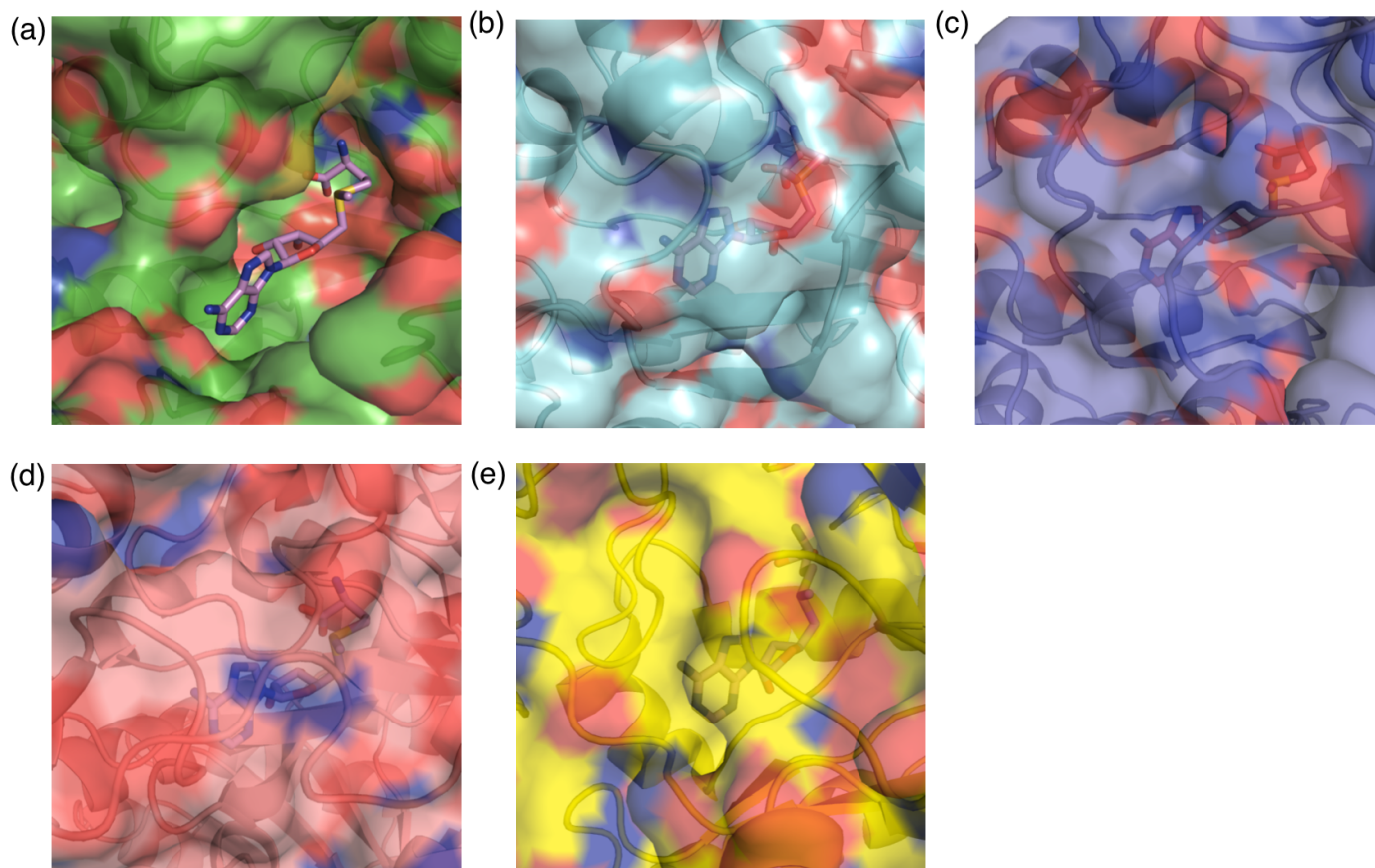


Figure S6. Structural Comparison of Radical SAM Enzymes. Surface representations of the active sites of radical SAM enzymes. Illustrated are the SAM-binding sites. (a) MoaA.² (b) Pyruvate formate-lyase activating enzyme (PFL-AE)³. (c) [Fe-Fe] Hydrogenase maturase protein, HydE.⁴ (d) Lysine 2,3-aminomutase (LAM).⁵ (e) Biotin synthase (BioB).⁶

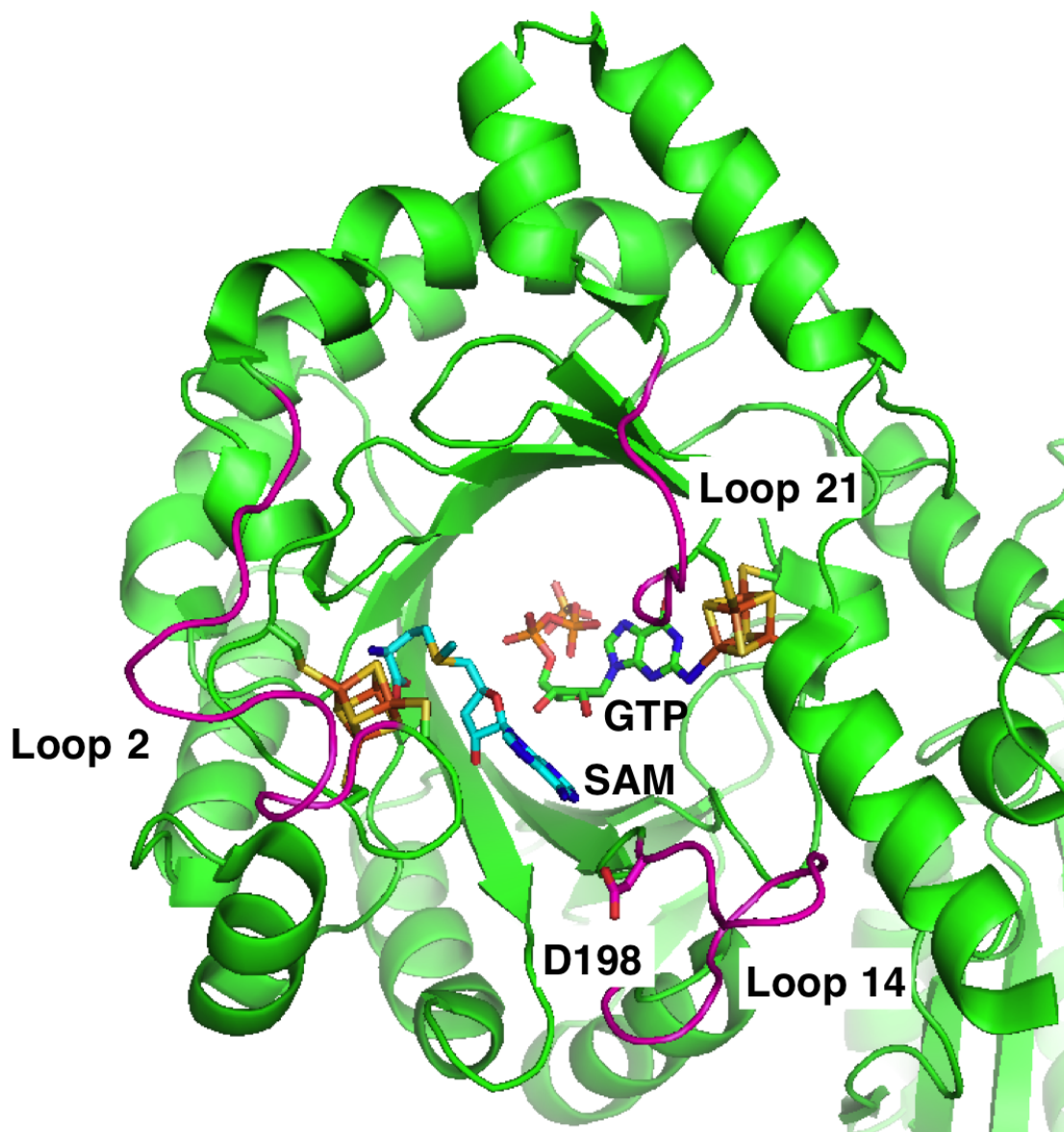


Figure S7. Loops around the active-site of MoaA. Loops that could be used to close the active-site are highlighted in red. Also shown are SAM, GTP, 4Fe-4S clusters and D198. SAM was modeled into the crystal structure of MoaA in complex with GTP (PDB ID: 2FB3)⁷ based on the crystal structures of MoaA in complex with SAM (PDB ID: 1TV8).²

Table S1. Complete List of the Steady State Kinetic Parameters for MoaA mutants.

Enzyme	Peptide (μM)	Substrate	K_m (μM) ^a	k_{cat} (min^{-1}) ^a	K_d (μM) ^a
MoaA Wt	0	GTP	3.1 ± 0.67	0.042 ± 0.005	5.0 ± 3.0
	0	SAM	5.1 ± 1.4	0.045 ± 0.007	1.7 ± 0.6
MoaA Δ 330-340	0	GTP	N.D. ^b	N.D. ^b	- ^c
	500		36 ± 8.7	0.023 ± 0.002	- ^c
	0	SAM	N.D. ^b	N.D. ^b	- ^c
500	57 ± 5.4		0.021 ± 0.001	- ^c	
MoaA G339A	0	GTP	N.D. ^b	N.D. ^b	0.46 ± 0.01
	500		19 ± 1.8	0.045 ± 0.006	- ^c
	0	SAM	N.D. ^b	N.D. ^b	$> 90^d$
500	34 ± 2.7		0.046 ± 0.004	- ^c	
MoaA G339S	0	GTP	N.D. ^b	N.D. ^b	- ^c
	500		19 ± 3.3	0.050 ± 0.003	- ^c
	0	SAM	N.D. ^b	N.D. ^b	- ^c
500	65 ± 14		0.055 ± 0.006	- ^c	
MoaA G340A	0	GTP	N.D. ^b	N.D. ^b	5.2 ± 2.3
	500		7.7 ± 3.8	0.047 ± 0.003	- ^c
	0	SAM	N.D. ^b	N.D. ^b	$> 90^d$
500	37 ± 14		0.037 ± 0.006	- ^c	
MoaA G340S	0	GTP	N.D. ^b	N.D. ^b	- ^c
	500		52 ± 10	0.048 ± 0.004	- ^c
	0	SAM	N.D. ^b	N.D. ^b	- ^c
500	89 ± 12		0.051 ± 0.004	- ^c	
D198A-MoaA	0	GTP	6.9 ± 0.73	0.0046 ± 0.0015	- ^c
	0	SAM	36 ± 6.9	0.0039 ± 0.00074	- ^c
R330A, K331A, K332A-MoaA	0	GTP, SAM	- ^c	0.0043 ± 0.0004	- ^c
	800	GTP, SAM	- ^c	0.035 ± 0.002	- ^c

^a Determined by the coupled assay with *S. aureus* MoaC and HPLC analysis of cPMP. K_d determined by anaerobic ITC. ^b No detection. The amount of cPMP formation was below the limit of detection. ^c Not determined. ^d Below the limit of detection for ITC analysis, $90 \mu\text{M}$.

Table S2. PCR Primers for MoaA GG Motif Mutants.

Primer	Sequence (5' to 3')
Δ330-340	GTTGCCAATCGTCAATAACGTAAAAAGATAAACATG
Δ336-340	CAACGTAAAAAGATAAACATGTAATATATTGGTGGTTAATG
D198A	GAATTTATGGCGGTTGGTAATGATAATG
D206A	GATAATGGATGGGCGTTCAGTAAAGTTG
D98A	GATGGTATTGAAGCGATTGGTTTGAC
E97A	CGATGGTATTGCGGATATTGGTTTG
G339A	CATGAATTATATTGCGGGTTAATGTGTAGG
G339S	CATGAATTATATTAGCGGTTAATGTGTAGG
G339V	CATGAATTATATTGTTGGTTAATGTGTAGG
G340A	GAATTATATTGGTGCGTAATGTGTAGGGAC
G340S	GAATTATATTGGTAGCTAATGTGTAGGGAC
G340V	GAATTATATTGGTGTTTAATGTGTAGGGAC
K331A	CAATCGTCAACGTGCGAAGATAAACATG
K332A	CAATCGTCAACGTAAAGCGATAAACATG
R330A	GCCAATCGTCAAGCGAAAAAGATAAAC
R330A-->R330A,K331A,K332A	CAATCGTCAAGCGGCAGCGATAAACATG

References

- (1) Hover, B. M.; Lokszejn, A.; Ribeiro, A. A.; Yokoyama, K. *J Am Chem Soc* **2013**, *135*, 7019-7032.
- (2) Hänzelmann, P.; Schindelin, H. *Proc Natl Acad Sci U S A* **2004**, *101*, 12870-12875.
- (3) Vey, J. L.; Yang, J.; Li, M.; Broderick, W. E.; Broderick, J. B.; Drennan, C. L. *Proc Natl Acad Sci U S A* **2008**, *105*, 16137-16141.
- (4) Nicolet, Y.; Amara, P.; Mouesca, J. M.; Fontecilla-Camps, J. C. *Proc Natl Acad Sci U S A* **2009**, *106*, 14867-14871.
- (5) Lepore, B. W.; Ruzicka, F. J.; Frey, P. A.; Ringe, D. *Proc Natl Acad Sci U S A* **2005**, *102*, 13819-13824.
- (6) Berkovitch, F.; Nicolet, Y.; Wan, J. T.; Jarrett, J. T.; Drennan, C. L. *Science* **2004**, *303*, 76-79.
- (7) Hänzelmann, P.; Schindelin, H. *Proc Natl Acad Sci U S A* **2006**, *103*, 6829-6834.